

**Best  
Available  
Copy**

AD-783 462

CIRCUITS FOR A PULSED DOPPLER RADAR

John Speulstra

Harry Diamond Laboratories

Prepared for:

Advanced Research Projects Agency

May 1974

DISTRIBUTED BY:

**NTIS**

**National Technical Information Service  
U. S. DEPARTMENT OF COMMERCE  
5285 Port Royal Road, Springfield Va. 22151**

The findings in this report are not to be construed as an official Department of the Army position unless so designated by other authorized documents.

Citation of manufacturers' or trade names does not constitute an official endorsement or approval of the use thereof.

Destroy this report when it is no longer needed. Do not return it to the originator.

REVISION BY	
DATE	With Service <input checked="" type="checkbox"/>
INFO	Self Service <input type="checkbox"/>
NAME	<input type="checkbox"/>
SIGNATURE	
APPROVAL	
RESPONSIBILITY	
DATE	
FILE	

UNCLASSIFIED

SECURITY CLASSIFICATION OF THIS PAGE (When Data Entered)

AD-783462

REPORT DOCUMENTATION PAGE		READ INSTRUCTIONS BEFORE COMPLETING FORM
1. REPORT NUMBER HDL-TM-74-8	2. GOVT ACCESSION NO.	3. RECIPIENT'S CATALOG NUMBER
4. TITLE (and Subtitle) Circuits for a Pulsed Doppler Radar		5. TYPE OF REPORT & PERIOD COVERED Technical Memorandum
		6. PERFORMING ORG. REPORT NUMBER
7. AUTHOR(s) John Speulstra		8. CONTRACT OR GRANT NUMBER(s) ARPA Order No. 1106
9. PERFORMING ORGANIZATION NAME AND ADDRESS Harry Diamond Laboratories Washington, D. C. 20438		10. PROGRAM ELEMENT, PROJECT, TASK AREA & WORK UNIT NUMBERS Project Element-6.27.02.D
11. CONTROLLING OFFICE NAME AND ADDRESS Director Defense Advanced Research Projects Agency 1400 Wilson Blvd., Arlington, VA 22209		12. REPORT DATE May 1974
		13. NUMBER OF PAGES 30
14. MONITORING AGENCY NAME & ADDRESS (if different from Controlling Office)		15. SECURITY CLASS. (of this report) UNCLASSIFIED
		15a. DECLASSIFICATION DOWNGRADING SCHEDULE
16. DISTRIBUTION STATEMENT (of this Report) Approved for Public Release; Distribution Unlimited		
17. DISTRIBUTION STATEMENT (of the abstract entered in Block 20, if different from Report)		
18. SUPPLEMENTARY NOTES AMCMS Code 5910.22.63373 HDL Project No. 121211 Report accepted October 9, 1973.		
19. KEY WORDS (Continue on reverse side if necessary and identify by block number) Goubau line personnel detection pulsed-doppler radar system low noise video amp tunable active filter range gate isolation		
20. ABSTRACT (Continue on reverse side if necessary and identify by block number) This report describes in detail the circuitry of a multirange-gate pulse doppler radar which operates at 500 MHz. The system is a low power one that generates only a one-watt (peak) pulse of 50 ns length at a 40 kHz rate, for an average power of 2 mW. The receiver employs RF amplification, a wide-band video amplifier following the coherent mixer, a set of boxcars used as range gates, and active high-pass filters which are voltage adjustable. The timing circuit required is discussed.		

DD FORM 1 JAN 73 1473 EDITION OF 1 NOV 65 IS OBSOLETE

1 UNCLASSIFIED  
SECURITY CLASSIFICATION OF THIS PAGE (When Data Entered)

TABLE OF CONTENTS

<u>Section</u>	<u>Title</u>	<u>Page</u>
1	INTRODUCTION . . . . .	5
2	BLOCK DIAGRAM DESCRIPTION . . . . .	5
3	PROCEDURE FOR DETERMINING RECEIVER RF GAIN . . . . .	7
4	DESIGN CALCULATIONS FOR RF GAIN . . . . .	7
5	THE VIDEO AMPLIFIER DESIGN AND ANALYSIS . . . . .	8
6	BUFFER SAMPLE AND HOLD . . . . .	10
7	FILTER DESIGN . . . . .	12
8	THE VARIABLE ACTIVE FILTER . . . . .	14
9	CONTROL OF THE VARIABLE ACTIVE FILTER . . . . .	18
10	ADDITIONAL DOPPLER PROCESSING CIRCUITS . . . . .	21
11	THRESHOLD CIRCUIT . . . . .	22
12	PULSE AND RANGE GATE GENERATOR . . . . .	22
13	CONCLUSION . . . . .	26
	ACKNOWLEDGEMENTS . . . . .	27
	LITERATURE CITED . . . . .	27
	APPENDIX A . . . . .	29

LIST OF ILLUSTRATIONS

<u>Figure</u>		
1	Pulsed-doppler radar block diagram . . . . .	5
2	Local oscillator . . . . .	6
3	Power amplifier . . . . .	6
4	Video amplifier output-response for various coupling methods . . . . .	9
5	Mixer video amp . . . . .	10
6	Complementary emitter follower . . . . .	10
7	Improved isolation emitter follower using FET current sources . . . . .	11
8	Sample and hold . . . . .	12
9	Variable four-pole high-pass Butterworth filter . . . . .	17
10	One of four MOSFET switches (RCA CD4016) . . . . .	17
11	Variable duty cycle multivibrator . . . . .	18
12	Improved multivibrator . . . . .	19
13	Voltage controlled monostable multivibrator . . . . .	20
14	Monostable waveforms . . . . .	20
15	Improved monostable multivibrator . . . . .	21
16	Duty/factor/pulse width - usec . . . . .	21
17	Doppler processor . . . . .	22
18	Threshold and latch . . . . .	23
19	Pulse generator . . . . .	24

## 1. INTRODUCTION

This report presents the design features of a pulsed-doppler radar. In particular it emphasizes the circuitry that processes the doppler signal. Some mention also will be made of the rf components.

Although the information in this report concerns only a particular pulsed-doppler radar, there may be many other applications where the information might be useful. For example, such items as the video amplifier, the sampling gate, and the active filters, are germane to many radar systems.

## 2. BLOCK DIAGRAM DESCRIPTION

Shown in figure 1 is the block diagram of a pulsed-doppler radar.

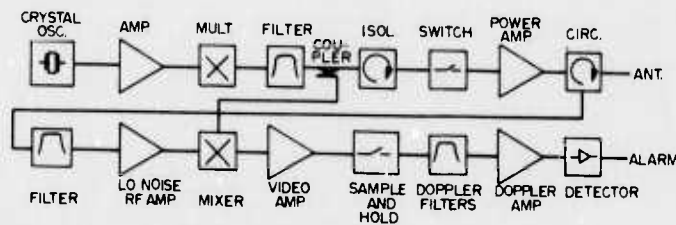


Figure 1. Pulsed-doppler radar block diagram.

The basic source for the system is a two-stage 125 MHz crystal oscillator. The crystal operates in the series mode and in the fifth overtone (fig. 2). The output of oscillator is buffered before amplification in class "A" and class "C" tuned stages. The output of the class "C" stage drives a pulse-forming network which prepares the signal for multiplication by the step-recovery-diode (SRD). The output of the SRD is tuned to maximize the fourth harmonic. The output power follows the  $P/n$  rule, where  $P$  is the class "C" output power and  $n$  is the multiplication factor. For this system as shown in figure 2, the output power was approximately 250 mW. The SRD action is described in reference 1. A five-pole-bandpass filter following the multiplier removes the unwanted harmonics. Local oscillator power for the receiver-mixer is taken from the sidearm of a directional coupler.

An isolator is used to isolate the cw circuitry from the subsequent pulse circuitry. A pulse generator drives the pin diode switch to produce the necessary pulse width and repetition rate. Following the switch, the pulse power is increased to a one-watt-peak-level in a class "C" amplifier (see figure 3). The output of the amplifier is passed via a circulator to the antenna.

<sup>1</sup>R. Neville, C. Forge, S. Hamilton, "Research and Development on Step Recovery Diodes, Pulse Generators, and Multipliers," HDL-TR-98(D), April 1967.

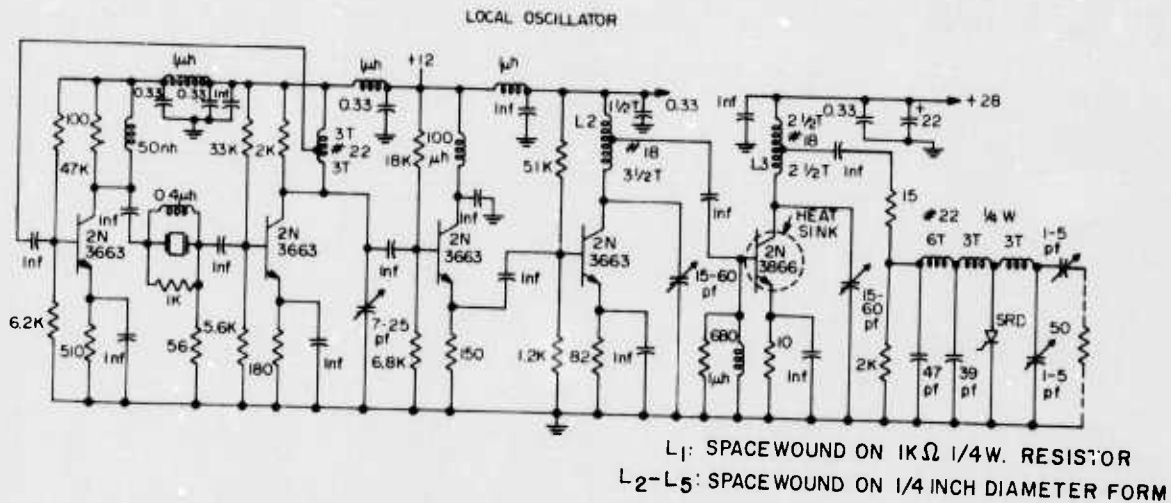


Figure 2. Local oscillator.

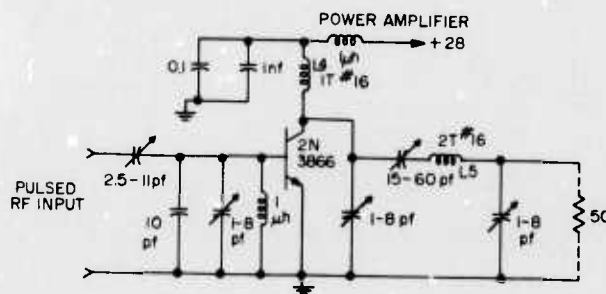


Figure 3. Power amplifier.

The received signal taken from the third terminal of the circulator is amplified in a low-noise amplifier. The amplifier has 24 dB of gain and a 3.7 dB noise figure. This noise figure ideally sets the signal-to-noise ratio for the complete receiver. The output of the amplifier connects to a filter (identical to the one previously mentioned). This is used to eliminate all-out interfering band signals from the signal port of a doubly-balanced mixer.

Most of the rf components mentioned (filter, isolator, directional coupler, circulator, rf amplifier and mixer) are readily available commercially; however, some items, particularly the rf switch is not. The pulse and bias ports were not designed with adequate rf shielding and as a result a large amount of cw-rf-power is radiated. The switch was enclosed in a rf-tight-box and rf filtering was introduced on both the pulse and bias ports. This alleviated this problem.

Following the mixer, the signal is processed for doppler information by a video amplifier, a group of sample-and-hold circuits, active filters, and thresholding circuits. A description of that part of the system will be given in detail. Before going into that detail some explanation is warranted on the procedure used to determine the required rf gain.

### 3. PROCEDURE FOR DETERMINING RECEIVER RF GAIN

In general, two main factors determine the gain:

1. The maximum gain of the amplifier can be determined by calculating the maximum clutter signal expected and assuring that this signal will not saturate the rf amplifier or the mixer following the amplifier. The doppler signal would be lost were saturation permitted.
2. The minimum gain can be approximated from the receiver-noise-figure calculations. There must be sufficient gain in the rf amplifier so that succeeding stages do not appreciably add to the overall noise figure. The following expression defines the overall noise figure:

$$N.F. = F_1 + (F_2 - 1)/G_1 G_2 + \dots$$

Where  $F_1, F_2$  etc. are the individual noise figures of the stages and  $G_1, G_2$  etc. are the gains.

### 4. DESIGN CALCULATIONS FOR RF GAIN

	KT = -174 dBm
25 MHz bandwidth (50 nsec pulse)	= 74 dB
	<hr style="width: 50%; margin-left: auto; margin-right: 0;"/> -100 dBm
Approx. noise figure	= 5 dB
	<hr style="width: 50%; margin-left: auto; margin-right: 0;"/> - 95 dBm
Required SCV*	= 70
	<hr style="width: 50%; margin-left: auto; margin-right: 0;"/> - 25 dBm

The maximum signal into the mixer should not exceed zero dBm. Therefore, the maximum rf gain should be about 25 dB.

An available transistor rf amplifier had the following specifications:

rf gain - 24 dB	1dB Gain Reduction - ODBM
Noise figure - 3.7 dB	Bandwidth 300 -- 500 MHz

To see how these specifications affect the overall noise figure the following calculations are shown:

---

\*Sub clutter visibility



rf amp & circulator	----	$F_1 = 3.7 \text{ dB} + 0.5 \text{ dB} = 4.2 \text{ dB}$ -- 2.63
Filter, mixer, video amplifier	----	$F_2 = 1 \text{ dB} + 6 \text{ dB} + 12 \text{ dB} =$ $19 \text{ dB} \text{ -- } 80 \text{ } G_1 = 24 \text{ dB} \text{ -- } 250$
		N.F. = $2.63 + 79/250 + \text{small}$ insignificant terms = $2.63 + 0.3$ = 2.93 = 4.7 dB

This indicates a degradation of only 0.5 dB, and a satisfactory amplifier for the purpose.

## 5. THE VIDEO AMPLIFIER DESIGN AND ANALYSIS

The design of the video amplifier is based upon the characteristics of the signal it must amplify, on source and load characteristics, and on the available dc power source. These are then used to determine bandwidth, coupling, gain, impedances, voltage swing, and noise figure of the amplifier. Since most of these parameters are not independent, some compromise must be made. How the above factors are related and the way they are used in the design of the amplifier will be shown below.

### 5.1 Bandwidth-coupling

The upper limit of frequency response is determined from the required preservation of pulse-rise-and-fall time or of pulse amplitude. The formula that relates pulse rise time to bandwidth is given by  $f_{BW} = 0.35/t_r$  where  $f$  is in Hz and  $t_r$  (rise time) in seconds (ref 2). If amplitude is preserved then  $f_{bw} = 1/t_{pw}$  where  $f$  is in Hz and  $t_{pw}$  (pulse width) is in seconds.

The lower limit of the frequency response is based upon pulse droop and pulse repetition rate. In most radar systems the video amplifier must provide the signal to a number of range gates and the isolation achieved between range gates depends upon the low-frequency response of the video amplifier. The maximum isolation is achieved if the amplifier responds down to dc. The maximum isolation achievable using ac coupling depends on the ratio of pulse-width to pulse-repetition rate or duty cycle. Figures 4,a,b,c show the response of the amplifier with ac and dc coupling.

If ac coupling is used, variations in amplitude of the pulse, as happens when a doppler signal is present, shows up as amplitude variation in the baseline. This is true because the average voltage must be zero. As can be seen from figure 4-d, poor low-frequency response results in poor

<sup>2</sup>J. Millman, H. Taub, "Pulse, Digital, and Switching Waveforms," McGraw-Hill, New York, 1965.

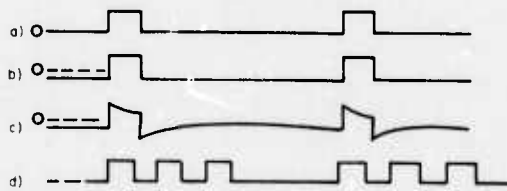


Figure 4. Video amplifier output-response for various coupling methods.

- a) dc coupled amplifier - maximum isolation
- b) ac coupled amplifier - best isolation achievable
- c) ac coupled amplifier - poor low-frequency response  
poor isolation
- d) Possible range gate configuration.

isolation, especially close to the received pulse. Of course, these problems do not exist in the dc-coupled case and maximum isolation is achieved. The relationship of pulse droop to the lower 3 dB frequency response and to the range gate isolation is derived in appendix A.

#### 5.2 Gain-Impedance-Voltage Swing

The gain of the video amplifier can be determined from the maximum output signal from the mixer and the maximum-input signal into the sample and hold circuit. The maximum mixer-output signal occurs each time a pulse is transmitted and is reflected from the antenna's VSWR back into the receiver. This is a large signal which saturates the rf amplifier and mixer. Generally these high-frequency components recover rapidly and cause no problem; however, the video amplifier is a relatively low-frequency device and its recovery is slow. Therefore, to avoid blocking the subsequent doppler signals, saturation of the video amplifier should not occur. The maximum output voltage from a balanced hot-carrier-diode mixer is approximately  $\pm 0.2$  Volt. The maximum input signal to the sample and hold is  $\pm 6$  V. Therefore, the maximum gain should be  $6 \text{ V}/0.2 \text{ V} = 30$ , or approximately 30 dB. Then, for a safety margin, the amplifier should have a minimum of  $\pm 7$  V output-voltage capability.

For an amplifier with the above capabilities the circuit of figure 5 was designed. This is a differential-input, single-ended, output amplifier and is dc coupled throughout. The open-loop gain is sufficient so that the ratio of the feedback resistor to the input resistor determines the gain. A single RC time constant sets the upper frequency limit. Either ac or dc coupling can be used at both input and output with the restrictions noted above. The complementary output stage can provide  $\pm 7$  V output swing into a 50 ohm load. For the amplifier to have a reasonable noise figure (one not to degrade front-end noise), the source impedance should be greater than 200 ohms. However, the optimum termination for the mixer is 50 ohms; therefore, a 100 ohm resistor was

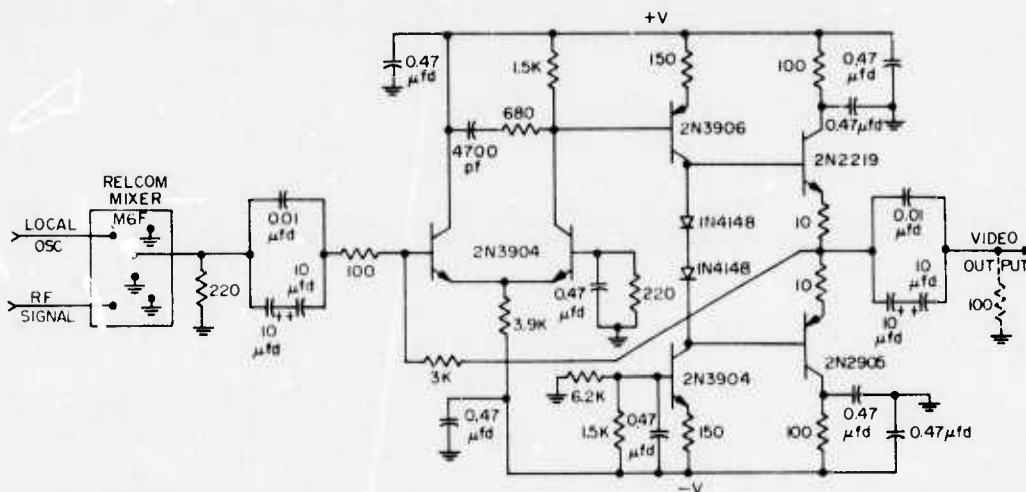


Figure 5. Mixer video amp.\*

used as an acceptable compromise. For very low-noise application, low-loss, input-matching circuits, such as rf chokes, a transformer, or inductive-capacitive elements, might be used. These are difficult to design with adequate bandwidths (ref 3).

#### 6. BUFFER SAMPLE AND HOLD

The output of the video amplifier is fed into a number of sample-and-hold circuits. To achieve good isolation between them, a buffer amplifier is required. This also lessens the drive requirements for the video amplifier and provides a low-impedance drive for the sample-and-hold circuitry. Normally, a standard emitter follower is sufficient; however, for large bipolar signals, complementary emitter followers are required. Figure 6 shows the emitter followers with their resistor biasing.

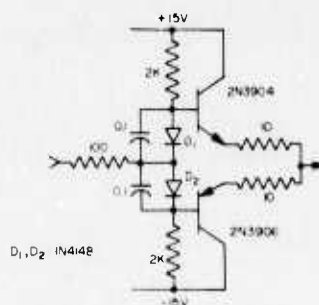


Figure 6. Complementary emitter follower.

<sup>3</sup>"Linear Integrated Circuits," RCA Technical Series IC-42, 1970.

\*An earlier design of the mixer video amplifier had a 44 MHz bandwidth and a 30 dB gain. It used 2N3261's in place of the 2N3904's, a 2N3250 in place of the 2N3906, a 2N3553 in place of the 2N2219, and a 2N5583 in place of the 2N2905. As only a lower bandwidth was required in the system, the transistors shown in figure 5 were substituted for the more costly transistors. The remainder of the components remained unchanged.

The drawback in this biasing method is that the power-supply rejection is poor whenever the signal is driven from a source having a fairly high output impedance at low frequencies. The ratio of source resistance, to the sum of source resistance and bias resistance, determines the power-supply rejection. At low frequencies, very little can be accomplished with supply filtering since the required capacitor values become completely unrealistic. To overcome this limitation, the biasing resistors are replaced by current sources. Since a good current source exhibits a high output impedance, a high degree of isolation is obtainable. Figure 7 shows the modification using the current sources.

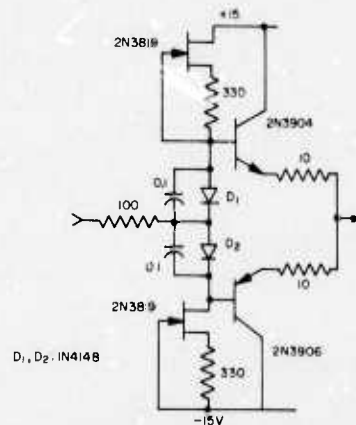


Figure 7. Improved isolation emitter follower using FET current sources.

The output from the buffer amplifier drives the sample-and-hold circuit. The parameters to consider include dynamic range, sampling time, hold time, biasing and isolation; figure 8 shows the circuitry. The sampling switch consists of an ultra-fast, low-capacitance, diode array. These diodes are fabricated on a common substrate to assure static and dynamic matching.

A pulse from the blocking oscillator forward biases the diodes, and samples the input waveform. In addition, the pulse stores charge on a capacitor, (in series with the diodes) which during the hold interval, reverse biases the diodes. The additional resistor and zener diode is used to limit the current and reverse voltage. This biasing scheme assures that large signals do not forward bias the diodes and modify the voltage on the holding capacitor. A pulse from the range-gate generator triggers the blocking oscillator which then generates a pulse of a fixed duration (ref 4). Pulse duration is set by the R and C components in the base circuit. Following the hold capacitor, a single pole, lowpass-filter removes switching transients. A high input-impedance amplifier follows the filter.

<sup>4</sup>John Markus, "Source Book of Electronic Circuits," McGraw-Hill, New York 1968.

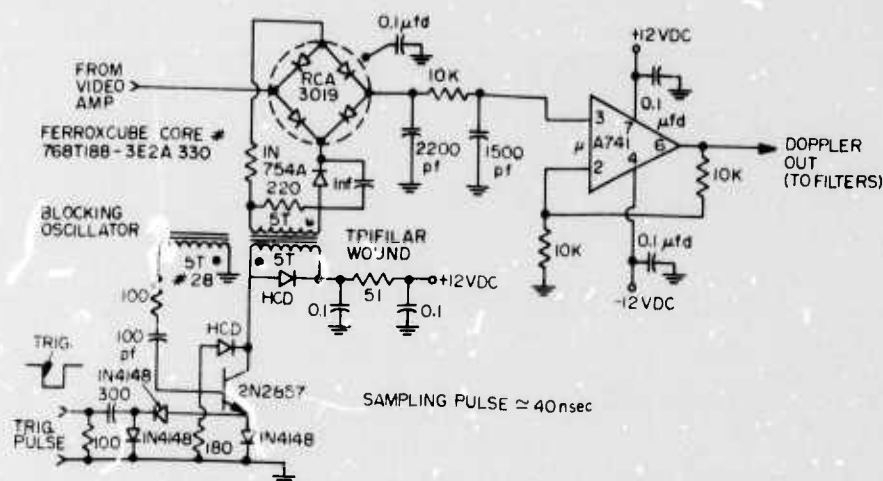


Figure 8. Sample and hold.

Excellent isolation is achieved by low-capacitance diodes and the self-biasing circuit. In addition, this biasing circuit provides a large dynamic range as well. The combination of low buffer-output impedance, low forward-diode resistance, and fast diodes permit rapid sampling of the input and fast charging of the holding capacitor. The maximum hold interval is governed by the reverse-diode leakage, the operational-amplifier bias current, and the value of the hold capacitor.

#### 7. FILTER DESIGN

One of the most important aspects of the radar design is the extraction of the signal in the presence of clutter. In the application of this system, the frequency content of the clutter was dependent on the action of wind upon the electromagnetic system and upon the vegetation. Therefore, to minimize the response with varying wind conditions, a tunable clutter filter had to be designed. An active filter was most attractive for the very low frequencies involved. Many articles in literature show the design of active filters but little is written about the design of a variable active filter. That being the case, a complete analysis is given in this report. (Recent literature, see refs 5,6,7,8,9)

<sup>5</sup>R. R. Shepard, "Active Filters: Part 12 Shortcuts to Network Design," *Electronics*, Vol. 42, No. 17, pp 82-91, August 18, 1969.

<sup>6</sup>F. W. Stephenson, "High-Pass Realization of Equal-valued Capacitor Active RC Networks," *Proceedings of the IEEE*, Vol. 60, No. 8, pp 996, August 1972.

<sup>7</sup>S. C. Dutta Roy, K. K. Malik, "Active RC Realization of a 3rd Order Low-Pass Butterworth Characteristic," *Electronic Letters*, Vol. 8, No. 26, 28 December 1972.

<sup>8</sup>R. G. Sparkes, A. S. Sedra, "Programmable Active Filters," *IEEE Journal of Solid State Circuits*, Vol. 5c-8, No. 1, pp 93-95, Correspondence, February 1973.

<sup>9</sup>L. T. Bruton, R. T. Pederson, "Tunable RC-Active Filters Using Periodically Switched Conductances," *IEEE Transactions on Circuit Theory*, Vol. CT-20, No. 3, pp 294-301, May 1973.

The transfer function for a two-pole, low-pass filter with gain "K" is

$$V_o/V_1 = \frac{K}{s^2 C_1 C_2 R_1 R_2 + s[C_2(R_1 + R_2) + C_1 R_1(1-K)] + 1.} \quad (1)$$

A fourth order, low-pass Butterworth characteristic was desired and this can be realized with

$$V_o/V_1 = \frac{K}{(s^2 + 0.7653s + 1)(s^2 + 1.847s + 1)}. \quad (2)$$

Separation of the denominator in Eq. 2, suggests that a four-pole filter can be realized as the cascading of two, two-pole filters. Treating each section separately and comparing the denominator coefficients of Eqs. 1 and 2 results in the following set of equations. (with  $C_1=C_2=1$  equal capacitor values)

$$\begin{aligned} R_1 R_2 &= 1 \\ (R_1 + R_2) + R_1(1-K) &= 0.7653 \end{aligned} \quad \begin{array}{l} \text{Section 1} \\ \end{array} \quad (3)$$

and

$$\begin{aligned} R_1 R_2 &= 1 \\ (R_1 + R_2) + R_1(1-K) &= 1.8477. \end{aligned} \quad \begin{array}{l} \text{Section 2} \\ \end{array} \quad (4)$$

It would also be convenient if the value of resistors could be made equal. Solving Eqs. 3 and 4 for  $R_1=R_2=1$  results in

$$\begin{aligned} 2 + (1-K) &= 0.7653 \\ K_1 &= 3 - 0.7653 = 2.2347 \end{aligned} \quad (5)$$

and

$$\begin{aligned} 2 + (1-K) &= 1.8477 \\ K_2 &= 3 - 1.8477 = 1.1523. \end{aligned} \quad (6)$$

This shows the gain ( $K_1, K_2$ ) required in each filter section. Notice how conveniently the value of K can be found directly from the coefficients of the terms in equation 2.

The pole distribution of a normalized Butterworth low-pass filter lies on a unit circle. The adjustment of "K" for each section of the filter merely rotates the poles on the unit circle. Thus the filter can be realized with several active networks. Equations similar to the previous ones, can be derived for high-pass filters, but this is unnecessary. The transformation from low-pass to high-pass filters is easily accomplished by interchanging resistors and capacitors.

In order to find the element values one must scale the resistor and capacitor values that were previously normalized. Therefore, it is necessary to divide capacitor values by  $2\pi f_c$  for frequency scaling and divide by "M" if the resistor values were scaled up by "M". Thus,  $f_c = \frac{1}{2\pi RC}$  cutoff frequency (ref 5).

## 8. THE VARIABLE ACTIVE FILTER

For our purpose an active adjustable filter was required. Among the methods that can be used to make an active filter variable are; a junction field effect transistor biased on a portion of its characteristics to simulate a variable resistance diode biased with current sources, lamp-photocell combination, analog multipliers, and RC multipliers. Each of these methods suffer from one or more of the following drawbacks: only a small signal capability, a requirement for accurate matching, slow response, non-linear response to the control voltage, changes due to temperature, and additional driver-circuitry requirements.

At the time we built the circuit (before the IC analog multiplier was available) the RC multiplier method seemed the most easily implemented. The RC multiplier method repetitively switches the resistor element of the filter into and out of the circuit. A variable duty cycle pulse is the controlling method. An analysis is given in section 8.1.

### 8.1 Analysis of the RC Multiplier

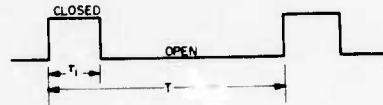
<u>Basic Circuit</u>	For Calculating Purposes the Equivalent Circuit is Used	<u>Equivalent Circuit</u>
----------------------	---	---------------------------



Where  $R_{EQ}$  is the Switched Resistance "R"

<sup>5</sup>R. R. Shepard, "Active Filters: Part 12 Shortcuts to Network Design," Electronics, Vol. 42, No. 17, pp 82-91, August 18, 1969.

Switch Operation - S



Conditions - The conditions that apply over the interval T are:

$$i_1 = V(t)/R \quad 0 \leq \tau \leq \tau_1. \quad (1)$$

$$i_1 = 0 \quad \tau_1 \leq \tau \leq T.$$

If the equivalent circuit is used and one solves for  $I_{ave}$

$$I_{ave} = \frac{1}{T} \int_0^T i_1 d\tau = \frac{1}{T} \int_0^{\tau_1} i_1 d\tau + \frac{1}{T} \int_{\tau_1}^T i_1 d\tau = \frac{1}{T} \int_0^{\tau_1} i_1 d\tau. \quad (2)$$

Now assume that  $i_1$  is constant over the interval T

$$I_{ave} = V/R_{EQ} = \frac{1}{T} \int_0^{\tau_1} V/R d\tau = \frac{V}{R} \frac{\tau}{T} \quad (3)$$

or

$$R_{EQ} = R \frac{T}{\tau_1}. \quad (4)$$

Thus, the equivalent resistance is equal to the fixed resistance, multiplied by the inverse of the duty cycle. The assumption that the current remains constant over the interval "T" is usually easily satisfied for low-frequency input signals. Consider for instance a high-pass Butterworth filter with a cut-off frequency of 5 Hz. Typical resistor and capacitor values are 15 K ohms and 2 $\mu$ fd, respectively. Then if one chooses a switching frequency of 10 kHz the conditions are easily satisfied. A frequency substantially higher than 10 kHz would have given a problem with the switching elements (MOSFETs).



An estimate of the error in the above assumption can be derived as shown below.

Let 
$$V(t) = V(1+at) - \text{input signal.} \quad (5)$$

Then 
$$V_{\text{ave}} = 1/T \int_0^T V(1+at) dt = V(1+aT/2) - \text{average input voltage.} \quad (6)$$

And 
$$I_{\text{ave}} = 1/T \int_0^{T_1} V(1+at)/R dt = \frac{V}{R} \left( T_1/T \right) \left( 1+aT_1/2 \right). \quad (7)$$

With the Solution 
$$R_{\text{EQ}} = V_{\text{ave}}/I_{\text{ave}} = \frac{V(1+aT/2)}{V/R T_1/T (1+aT_1/2)} =$$
  

$$= R T/t_1 \left[ 1 + \frac{(a/2)(T-t_1)}{1+a t_1/2} \right] \quad (8)$$

or 
$$R_{\text{EQ}} = (RT/t_1) (1 + \epsilon) \quad (9)$$

where 
$$\epsilon = \text{ERROR} = \frac{a/2 (T - t_1)}{1 + at_1/2} = \frac{T-t_1}{(2/a)t_1}. \quad (10)$$

For a specific value of "T" the maximum error occurs whenever  $t_1 \ll T$  and it is approximately equal to

$$\epsilon_{\text{max}} \approx aT/2 \quad (\text{since } 2/a \gg t_1 \text{ as will now be shown}). \quad (11)$$

In terms of a sine wave-input signal  $a = 2\pi/T_{\text{in}}$  (maximum slope) where  $T_{\text{in}}$  is the period of the input signal.

Then 
$$\epsilon_{\text{max}} = (2\pi/T_{\text{in}})T/2 = \pi T/T_{\text{in}}. \quad (12)$$

This shows that to keep the error small,  $\pi T \ll T_{\text{in}}$ .

If  $\pi T \ll T_{\text{in}}$  and  $t_1 \ll T$ .

Then

$$\pi t_1 \ll \pi T \ll T_{in}$$

Or

$$t_1 \ll T \ll T_{in}/\pi \quad \text{But } T_{in}/\pi = 2/a \therefore t_1 \ll T \ll 2/a$$

as was stated in equation 11.

The important result is that  $R_{EQ} = R T/t_1$ . For as shown previously  $f_c = 1/(2\pi R_{EQ}C)$  and combining these equations yields

$$f_c = t_1/(2\pi TRC).$$

Since the denominator is constant the cutoff frequency is directly proportional to  $t_1$  (switch on-time). Linear control of the cutoff frequency hence requires the pulse width to be linearly controlled. Circuits that have this capability are discussed later.

## 8.2 PRACTICAL FILTER

A practical realization of the above filter concept is shown in figure 9. It employs MOSFETs as the switching elements. These could be discrete transistors or a new MOSFET quad ICI switch such as the RCA CD4016 as reproduced in figure 10.

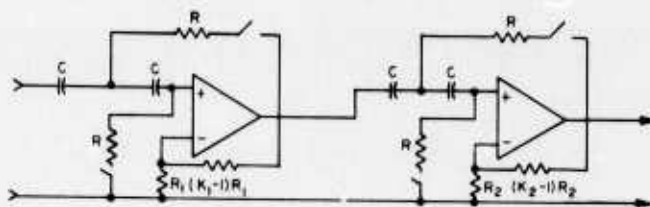


Figure 9. Variable four-pole high-pass Butterworth filter.

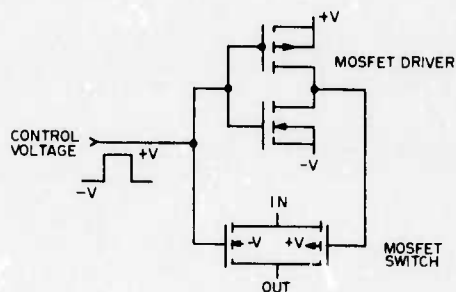


Figure 10. One of four MOSFET switches (RCA CD4016).

The advantage of using the IC quad switch is that it contains the built-in driver as well as input gate protection (not shown). Other advantages include: smaller size, switch "R<sub>on</sub>" resistance is closely matched and tracks with temperature, and the switch has capability to handle a large signal ( $\pm 7V$  with  $V_+ = 7, V_- = 7$ ). However, remember that "R<sub>on</sub>" must be considered as part of "R" as labeled in figure 9. It is best to make  $R \gg R_{on}$  so that any variation of R<sub>on</sub> has little influence on the filter. Another point is that the maximum value of  $R_{EQ} \ll 2R_{in}$  for a low-pass filter while  $R_{EQ} \ll R_{in}$  for a high-pass filter. Where R<sub>in</sub> is the closed loop input resistance (ref 5).

## 9. CONTROL OF THE VARIABLE ACTIVE FILTER

### 9.1 Multivibrator

The application of the filter will generally determine the type of control that is required. The controlling circuit could be a standard multivibrator or a voltage-controlled monostable circuit. A multivibrator configured for a variable duty-cycle operation is shown in figure 11 below.

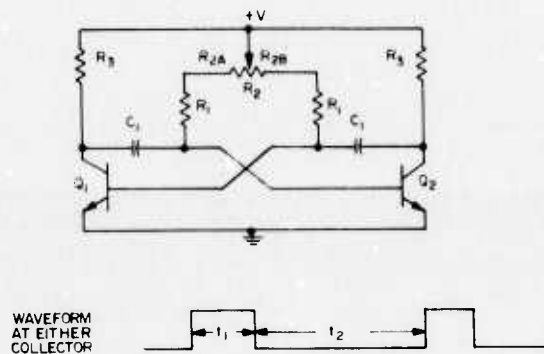


Figure 11. Variable duty cycle multivibrator.

$$\text{Calculations show that, } t_1 = (R_1 + R_{2A}) C_1 \ln (2V_{cc}/(V_{cc}-V_{BE})) \quad (1)$$

$$\text{and } t_2 = (R_1 + R_{2B}) C_1 \ln (2V_{cc}/(V_{cc}-V_{BE})) \quad (2)$$

$$\begin{aligned} \text{or that the period } t_1+t_2 &= C_1 \ln (2V_{cc}/(V_{cc}-V_{BE})) [R_1 + R_{2A} + R_1 + R_{2B}] \\ &= C_1 \ln (2V_{cc}/(V_{cc}-V_{BE})) [2R_1 + R_2] \end{aligned} \quad (3)$$

<sup>5</sup>R. R. Shepard, "Active Filters: Part 12 Shortcuts to Network Design," Electronics, Vol. 42, No. 17, pp 82-91, August 18, 1969.

Equation 3 shows that the period ( $t_1 + t_2$ ) is independent of the setting of  $R_2$ . The duty cycle can be calculated as follows:

$$\begin{aligned}
 t_1/t_1 + t_2 &= \frac{(R_1 + R_2A) C_1 \ln (2V_{cc}/(V_{cc}-V_{BE}))}{(2R_1 + R_2) C_1 \ln (2V_{cc}/(V_{cc}-V_{BE}))} \\
 &= \frac{R_1 + R_2A}{2R_1 + R_2} \cdot
 \end{aligned}
 \tag{4}$$

This shows that the duty cycle is directly proportional to the setting of  $R_2$ . The circuit as shown in figure 10 is limited to a linear duty-cycle range of approximately 20 to 80 percent. The limiting factors are: the recharging time of the capacitors, the base current limiting resistor  $R_1$ , and the reverse breakdown of the base-emitter junction. The addition of two transistors and diodes as shown in figure 12 offers a significant improvement to the operation of the circuit. The transistors provide a low-impedance path to recharge the capacitors, the two diodes in the base circuit prevent base-emitter breakdown, and the two remaining diodes provide a charging path for the capacitors. Not so obvious is the fact that the load resistor  $R_3$  can be changed to a higher value with the addition of the transistors and therefore the value of  $R_2$  may be increased. This results in greater linear range of operation than the previous unmodified circuit. However, no easy modification exists to make the duty cycle voltage controllable.

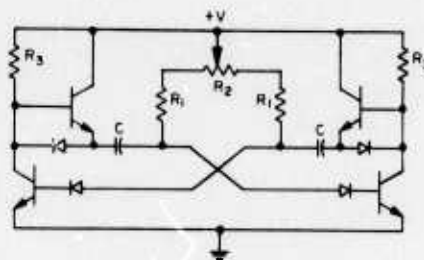


Figure 12. Improved multivibrator.

## 9.2 The Voltage Controlled Monostable Multivibrator

The advantage of using a monostable multivibrator to drive the filter is that the interference (referred to as walk-through) is avoided by synchronizing the monostable multivibrator to the PRF of the system, and that the pulse width can be voltage controlled. A circuit that accomplishes this is shown in figure 13. Since this is not a standard monostable multivibrator, the operation of the circuit will be described in detail.

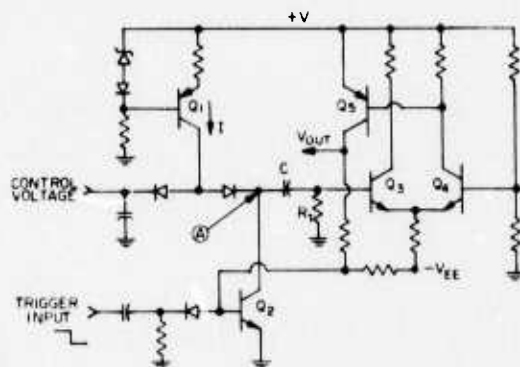


Figure 13. Voltage controlled monostable multivibrator.

### 9.3 Monostable Multivibrator Operation

Prior to a trigger pulse  $Q_2$ ,  $Q_4$ , and  $Q_5$  are turned on. The transistor  $Q_1$  is a constant current source. Upon the receipt of a negative-going trigger pulse,  $Q_2$  switches off and allows current to flow through  $C$  and  $R_T$ . The voltage developed across  $R_T$  exceeds the base voltage on  $Q_4$ . Therefore  $Q_3$  turns on and  $Q_4$  and  $Q_5$  turn off. Since  $Q_5$  turns off,  $Q_2$  is kept off by a resistor returned to  $V_{EE}$ . Since the capacitor  $C$  charges to a voltage equal to the control voltage, some current is diverted through the diode to the control input. The result is that the voltage reduces across  $R_T$ , thus  $Q_4$ ,  $Q_5$  and  $Q_2$  switch back on and this completes the cycle.

The fact that the capacitor is charged from a constant current source makes the circuit exhibit a very linear response of control voltage vs pulse width. The limitations that do occur, do so for very narrow pulses and pulses nearly equal to the input-trigger period. The waveforms in figure 14 illustrate these points.

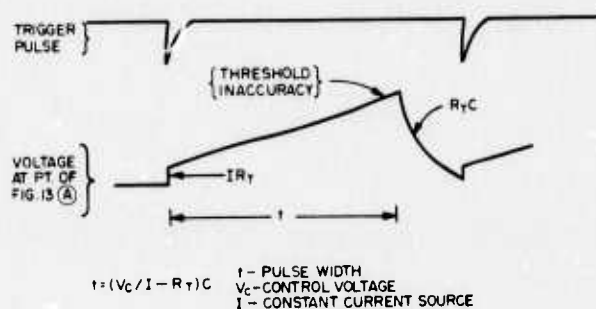


Figure 14. Monostable waveforms.

The inaccuracy of detecting the threshold prevents the generation of very narrow pulses, whereas the capacitor-discharge time limits the maximum pulse widths that can be generated. Considerable improvement can be made in both these areas with the addition of two tunnel diodes. Figure 15 indicates the modifications.

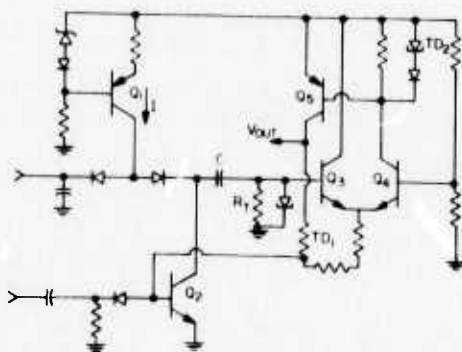


Figure 15. Improved monostable multivibrator.

The tunnel diode TDI enhances the  $Q_3$  turn-on but more importantly the discharge time is significantly reduced by means of the low impedance path of TDI. The addition of TD2 reduces the threshold inaccuracy by accurately sensing the current in  $Q_4$  and rapidly switching  $Q_5$  on. Figure 16 is a graph of control voltage vs output pulse width.

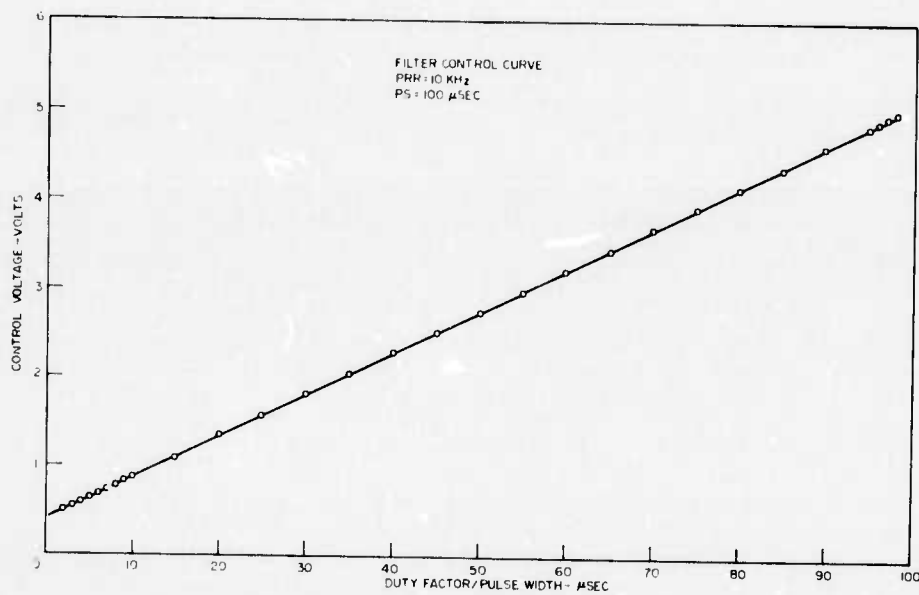


Figure 16. Duty/factor/pulse width -  $\mu$ sec

#### 10. ADDITIONAL DOPPLER PROCESSING CIRCUITS

Figure 17 shows the complete doppler-processor schematic. The variable-active filter and filter-driver circuits have already been discussed. The additional doppler processing circuitry will not be given in detail since these are standard amplifiers and filters. The captions shown in

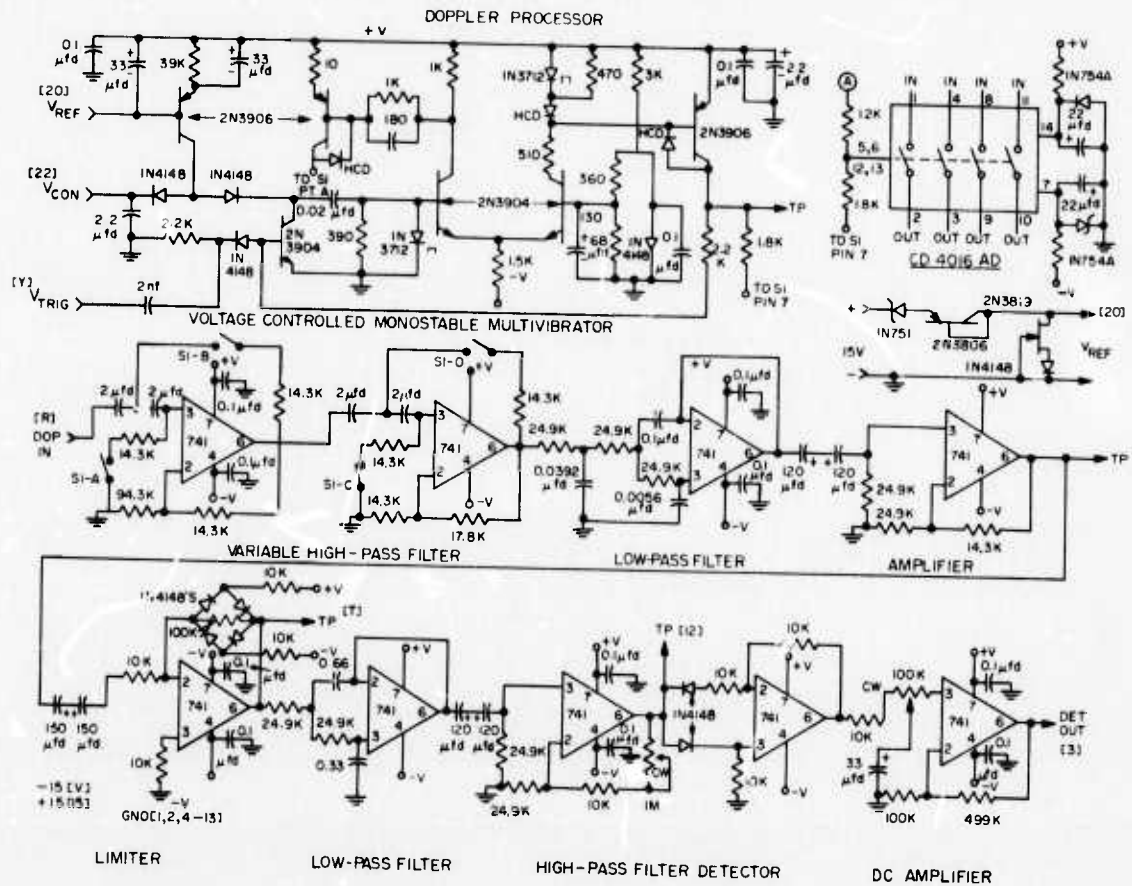


Figure 17. Doppler processor.

Figure 17 should suffice to show the function performed by each section. Outputs are provided as a means for recording the doppler signals as well as a dc level proportional to signal strength to drive the threshold circuits.

#### 11. THRESHOLD CIRCUIT

Figure 18 is the schematic of the threshold board. Direct current outputs of the doppler processor are compared to a preset dc-threshold level. Any signal exceeding the threshold level latches the circuit and drives a lamp. Reset is accomplished by reversing the bias applied to the input of the comparator. A standard operational amplifier is used as the comparator.

#### 12. PULSE AND RANGE GATE GENERATOR

The requirement that the range gates be variable, with respect to each other and as a group to the transmitted pulse, prompted the design of the range-gate generator as shown in figure 19. The generator is best

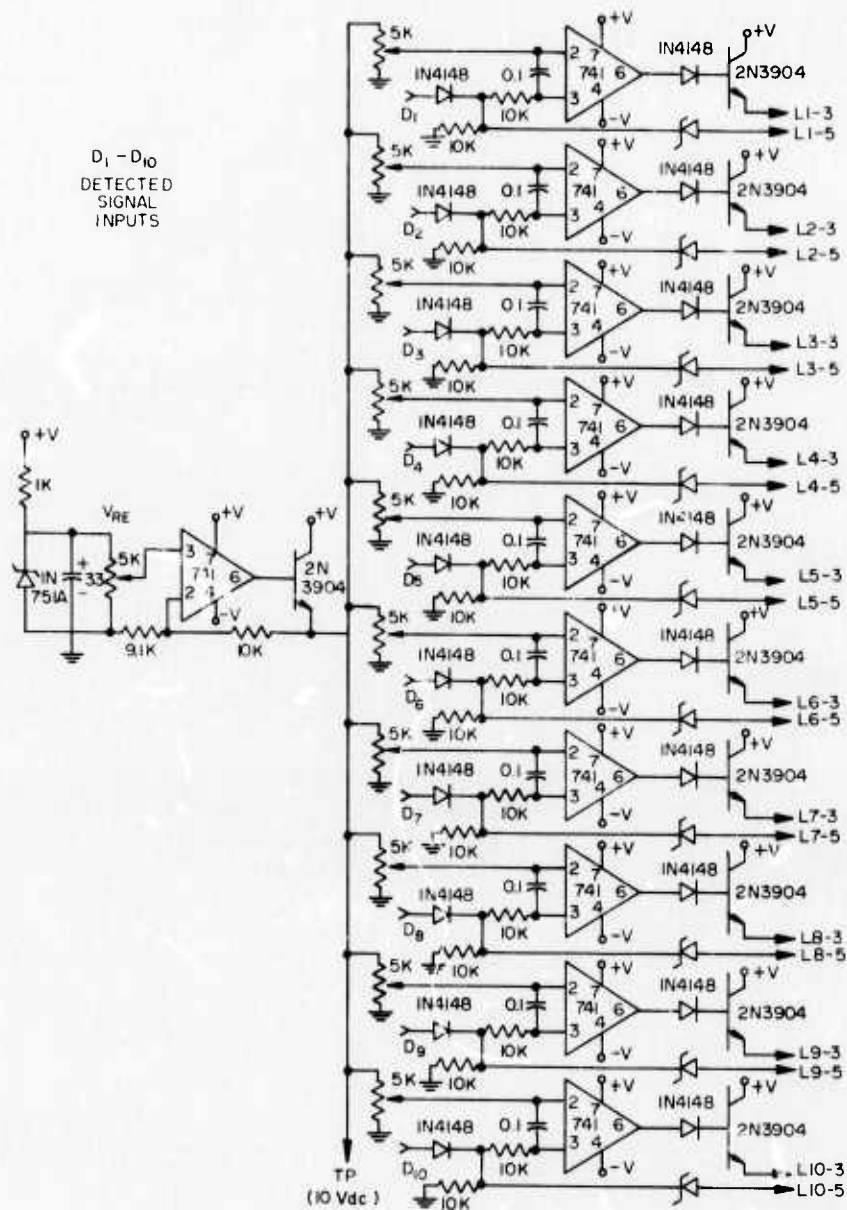


Figure 18. Threshold and latch.

described by considering the five functions that make up the generator. These are as follows: oscillator, triggered ramp generator, variable dc bias voltage, high-speed comparators, and the blocking oscillators.



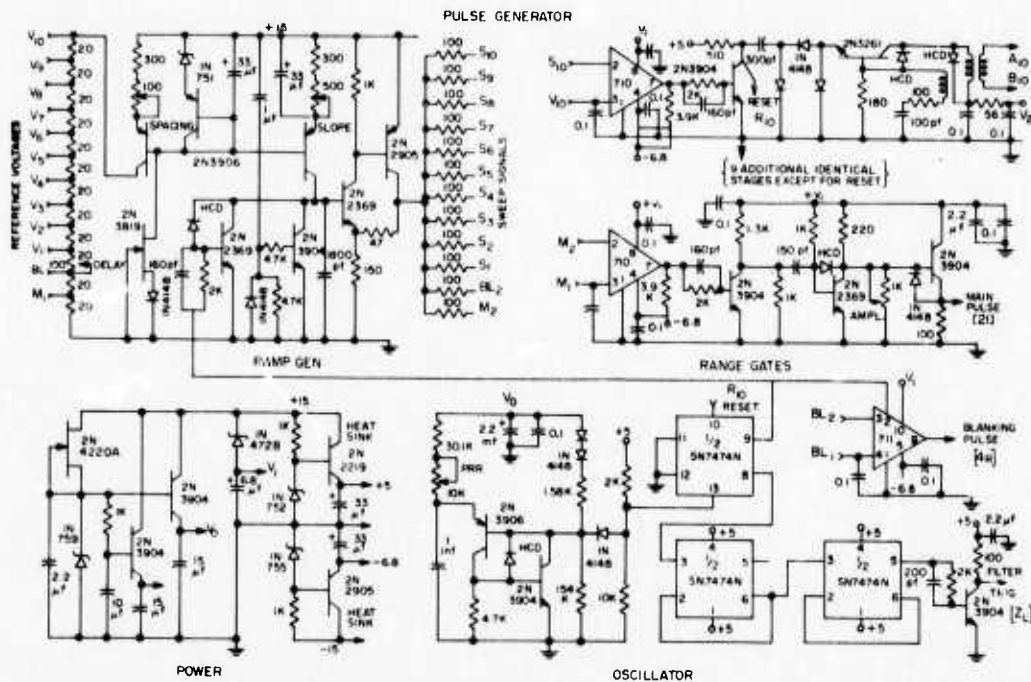


Figure 19. Pulse generator.

### 12.1 Oscillator

The basic timing is derived from a RC relaxation oscillator. The operation is similar to the popular unijunction oscillator (UJT). However, a little more flexibility is provided by using two transistors instead of the UJT. As was previously mentioned in section on buffer amplifiers, low frequency signals on supply lines are difficult to filter out; therefore, the oscillator is provided with a separate, regulated voltage. A constant current source (FET with low threshold voltage) biases a zener diode into its proper region to provide a stable reference voltage for the oscillator. The output of the oscillator triggers a bistable circuit which in turn controls the start of the ramp generator. In addition, the bistable drives a divide-by-four circuit which triggers the controls of the variable doppler filters.

### 12.2 Ramp Generator and Bias Supply

The ramp generator provides variable ramp and bias voltages for the comparators. To produce the ramp input, a current source linearly charges a capacitor for the up slope and a transistor switch rapidly resets it. A high-impedance buffer amplifier isolates the ramp voltage on the capacitor from the load. The bias voltages are developed across a series string of resistors driven from a current source. The resistors are closely matched to provide accurate and uniform spacing between range gates. Both the ramp and bias current sources are adjustable to give

the generator considerable flexibility. In addition, these sources use a common zener-diode reference-source for temperature and power supply compensation, Note, as in the case of the oscillator, the zener diode is biased with a FET-current source for addition supply isolation.

### 12.3 Comparators

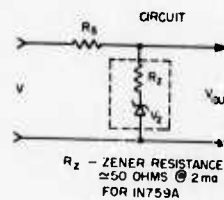
The high speed comparators compare the ramp voltage to the bias voltage and, whenever one exceeds the other, the state of the output changes. For a fixed bias voltage, the adjustment of the slope of the ramp causes a spacing change between the range gates. Similarly an adjustment in the biasing string of resistors provides a variable spacing between the transmitted pulse and the range gates. There are two more comparators than those required for the range gates; one provides a blanking pulse for the receiver, and the other, along with its monostable circuit, provides the transmitted pulse. In order to gain a better view as to the function of the five elements together, a summary of the operation is now given. An initial power-on reset is applied to the ramp generator capacitor (for a few milliseconds) to insure proper sequencing. In the meantime, a trigger pulse from the oscillator has set the bistable in a state to enable the ramp generation to proceed. As the capacitor charges and the ramp voltage is applied to the comparators, and in turn the output of each comparator changes state to produce the blanking, transmitting and range-gate pulses. The last comparator resets the bistable and in turn resets the ramp generator. The next oscillator trigger applied to the bistable enables the next cycle to commence.

It may also be helpful to show the advantage of using a current source to bias a zener diode instead of a resistor.

#### STANDARD RESISTOR BIASING

From the Circuit Diagram

$$\begin{aligned} V_{\text{out}} &= V_z + \left( \frac{V - V_z}{R_s + R_z} \right) R_z \\ &= V_z \left[ \frac{1 - R_z}{R_s + R_z} \right] + V \left( \frac{R_z}{R_s + R_z} \right) \\ &= V_z \left( \frac{1}{1 + R_z/R_s} \right) + V \left( \frac{1}{1 + R_s/R_z} \right) \end{aligned}$$

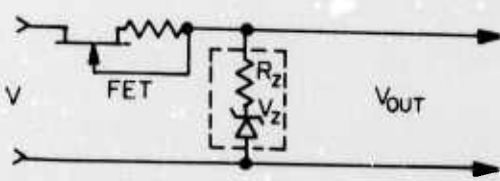


For a change in  $V$  of  $\Delta V$  then

$$\Delta V_{\text{out}} = \Delta V \left( \frac{1}{1 + R_s/R_z} \right) \quad (1)$$

### FET Current-Source Biasing

(Same equations as above except  $R_F$  is substituted for  $R_S$ )

$$\Delta V_{out} = \Delta V \left( \frac{1}{1 + R_F/R_Z} \right) \quad (2)$$


From equations 1 and 2 the sensitivity of  $V_{out}$  due to supply changes is

$$S_R = \frac{\Delta V_{out}}{\Delta V} = \frac{1}{1 + R_S/R_Z} \quad (3)$$

$$S_F = \frac{\Delta V_{out}}{\Delta V} = \frac{1}{1 + R_F/R_Z} \quad (4)$$

For a typical case of  $V = +15V$   $I_Z = 2ma$   $V_Z = 12V$

$$R_Z + R_S = \frac{15 - 12}{2} = 1.5K \quad R_F = 250K @ 2ma$$

Thus

$$\therefore S_R = \frac{1}{1 + 1500/5} = \frac{1}{1 + 30} = 1/31 = 0.032$$

and

$$S_F = \frac{1}{1 + 2500/50} = \frac{1}{1 + 5000} = .0002$$

or dB improvement by using FET is

$$= 20 \log 0.032/0.0002$$

$$= 44 \text{ dB}$$

### 13. CONCLUSION

The transmitter-receiver system described was part of an experiment to use a Goubau line for intrusion detection. This report was written to describe features of the system, particularly the clock, the video amplifier, and the active filters that might be of use in other equipments. As the whole program has recently been declassified, the transmitter-

receiver may now be discussed in the role for which it was built. After the few minor modifications were accomplished, as discussed above, it performed quite well. It had the subclutter visibility (S.C.V.) and sensitivity for which it was designed. The gates were well decoupled and the video amplifier has even more dynamic range than the 70 dB S.C.V. implied. The timing circuitry was reliable and flexible.

#### ACKNOWLEDGEMENTS

The useful comments and advice of Dr. William Saunders, and the mechanical layout and construction of the system by Simon J. Knaggs, is much appreciated.

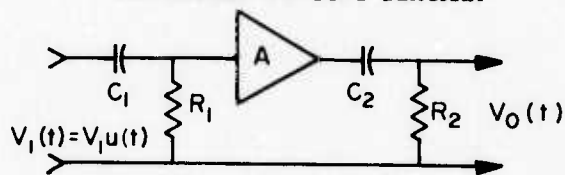
#### LITERATURE CITED

1. Neville, R., C. Forge, S. Hamilton, "Research and Development on Step Recovery Diodes, Pulse Generators, and Multipliers," HDL TR-98(D), April 1967.
2. Millman, J. and H. Taub, Pulse, Digital, and Switching Waveforms, McGraw-Hill, New York, 1965.
3. Linear Integrated Circuits, RCA Technical Series IC-42, 1970.
4. Markus, J., Source Book of Electronic Circuits, McGraw-Hill, New York, 1968.
5. Shepard, R. R., "Active Filters: Part 12 Shortcuts to Network Design," Electronics, Vol. 42, No. 17, pp 82-91, August 18, 1969.
6. Stephenson, F. W., "High-Pass Realization of Equal-valued Capacitor Active RC Networks," Proceedings of the IEEE, Vol. 60, No. 8, pp 996, August 1972.
7. Roy, S. C. Dutta, K. K. Malik, "Active RC Realization of a 3rd Order Low-Pass Butterworth Characteristic," Electronic Letters, Vol. 8, No. 26, 28 December 1972.
8. Sparkes, R. G., A. S. Sedra, "Programmable Active Filters," IEEE Journal of Solid State Circuits, Vol. 5c-8, No. 1, pp 93-95, Correspondence, February 1973.
9. Bruton, L. T., R. T. Pederson, "Tunable RC-Active Filters Using Periodically Switched Conductances," IEEE Transactions on Circuit Theory, Vol. CT-20, No. 3, pp 294-301, May 1973.

APPENDIX A

ANALYSIS OF INPUT AND OUTPUT COUPLING OF  
A VIDEO AMPLIFIER WITH A STEP INPUT VOLTAGE  $\mu(t)$

SIMPLIFIED CIRCUIT DIAGRAM



$$a = \frac{1}{R_1 C_1}$$

$$b = \frac{1}{R_2 C_2}$$

Case I  $a \neq b$

$$V_o(t) = \frac{AV_1}{a-b} [ae^{-at} - be^{-bt}]$$

Case II  $a = b$

$$V_o(t) = AV_1 e^{-at} (1-at)$$

for  $1 \ll b \ll 1$   $e^{-at} = (1-at)$

$$V_o(t) = \frac{AV_1}{a-b} [a(1-at) - b(1-bt)]$$

$$= \frac{AV_1}{a-b} (a - a^2 t - b + b^2 t)$$

$$= \frac{AV_1}{a-b} [(a-b) - t(a^2 - b^2)]$$

$$= AV_1 [1 - t(a+b)]$$

$$V_o(t) = AV_1 (1-at) (1-at)$$

$$= AV_1 (1 - 2at + a^2 t^2)$$

$$\approx AV_1 (1 - 2at)$$

Since  $a^2 t^2 \ll 2at$

Form a difference  $V_o(t=0) - V_o(t) = \Delta V(t)$

$$\Delta V(t) = AV_1 - AV_1 [1 - t(a+b)]$$

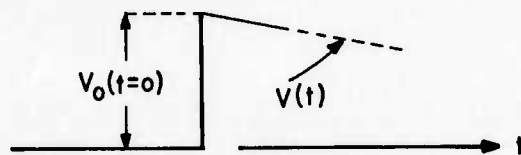
$$= AV_1 [1 - 1 + t(a+b)]$$

$$= AV_1 [t(a+b)] \quad (1)$$

$$\Delta V(t) = AV_1 - AV_1 (1 - 2at)$$

$$= AV_1 [1 - (1 - 2at)]$$

$$\Delta V(t) = AV_1 2at \quad (2)$$



In terms of relative droop - P

$$P = \frac{\Delta V(t)/2}{AV_1}$$

$$P = \frac{t(a+b)}{2} \quad \text{Case I} \quad (3)$$

$$P = at \quad \text{Case II} \quad (4)$$

To form a relationship between droop and lower 3dB freq. the derivation is as follows

$$\begin{aligned} V_o(\omega) &= AV_1(j\omega) \frac{R_1}{R_1 + 1/j\omega C_1} \cdot \frac{R_2}{R_2 + 1/j\omega C_2} \\ &= AV_1(j\omega) \frac{-\omega^2}{j\omega + 1/R_1 C_1} \frac{-\omega^2}{j\omega + 1/R_2 C_2} \\ &= AV_1(j\omega) \frac{-\omega^2}{(j\omega + a)(j\omega + b)} \\ &= AV_1(j\omega) \frac{-\omega^2}{-\omega^2 + j\omega(a+b) + ab} \\ &= AV_1(j\omega) \frac{-\omega^2}{-\omega^2 + ab + j\omega(a+b)} \end{aligned}$$

Squares amplitude response at  $\omega_{3dB}$

$$\frac{V_o(\omega)^2}{AV_1(\omega)^2} = \frac{\omega^4}{\omega^4 + \omega^2 a^2 + b^2 + a^2 b^2}$$

Solving for  $f_{3dB}$  we obtain

$$f_{3dB} = \frac{1}{2\pi} \sqrt{a^2 + b^2/2 + 1/2 \sqrt{(a^2 + b^2)^2 + 4a^2b^2}} \quad (5)$$

for  $a = b$

$$f_{3dB} = \frac{a}{2\pi} \sqrt{1 + \sqrt{2}} \quad (6)$$

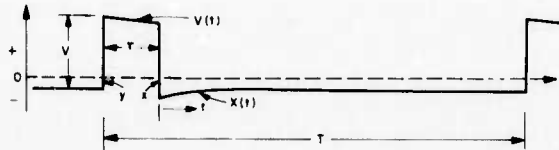
$$\approx 0.247a$$

and

$$P = \frac{\omega_{3dB} t}{\sqrt{1 + \sqrt{2}}} \quad (7)$$

In the presence of droop due to the ac coupling, the pulse response of the video amplifier possesses an accompanying "tail" which may cause feedthrough into the next range gate during the same PRF interval. An analysis of the feedthrough voltage causing this problem is now given

For a continuous pulse rate



Areas above and below zero must be equal, therefore for ideal ac coupling (no droop)

$$(V - y)\tau = y(T - \tau)$$

$$y = V \tau / T \quad \text{or} \quad \frac{y}{V} = \frac{\tau}{T} \quad (8)$$

Taking droop into account ( $a = \frac{1}{R_1 C_1}$ ,  $b = \frac{1}{R_2 C_2}$  Using Eqn. 2.

$$\Delta V(\tau) = V(a+b)\tau \quad \text{for } a\tau \ll 1 \quad b\tau \ll 1$$

$$\text{Then } X(t) = y + \Delta V(t) = V\tau/T + V(a+b)\tau[1 - (a+b)t]$$

$$\frac{X(t)}{V} \cong \frac{\tau}{T} + (a + b)\tau[1 - (a+b)t] \quad \{\text{for } (a+b)t < 1\}$$

or the feedthrough expressed in dB is

$$F = 20 \log \left| \frac{\tau}{T} + (a+b)\tau [1 - (a+b)t] \right| \quad (9)$$

Eqns. 8 & 9 are important in determining range gate isolation.